EP-DT
Detector Technologies

Radiation tolerance and annealing studies using test-structure diodes from 8-inch silicon sensors for CMS HGCAL

Leena Diehl (EP-DT-TP)

EP-DT Training Seminar
27 March, 2024
CERN

Outline

- Introduction to radiation damage and annealing
    - Types of radiation damage
    - Microscopic effects
    - Macroscopic effects
    - Annealing effects
- Introduction to HGCAL
- Experimental setup and measurements
- Pre-annealing results: Fluence dependence
- Ongoing study: Annealing behavior

Reminder: pn-junctions

Before contact

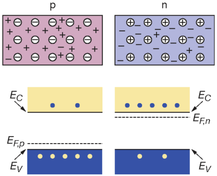

pn-junction

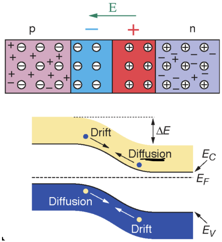

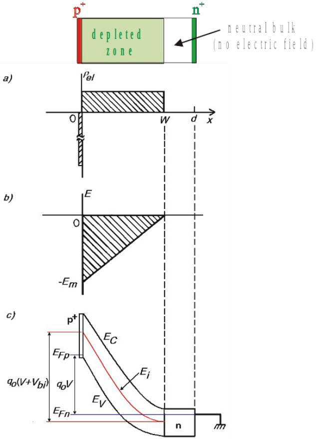

Electrical charge density

Electrical field strength

Electron potential energy

Reminder: Silicon sensors

Working Principle:

- pn-junction with external reverse voltage applied
- p-type: Additional acceptors → depleted: neg. space charge
- n-type: Additional donors → depleted: pos. space charge

p-type sensors: n-implants in a p-type bulk

- Electrons drift toward implants
- Holes drift toward backplane
- Drift velocity: $\vec{v} = \mu * \vec{E}$

Sensor characteristics:

- Full depletion voltage
- Leakage current
- Capacitance
- Charge collection efficiency

Effective doping concentration:

$$\left|N_{\text{eff}}\right| = \left|N_{\text{Donor}} - N_{\text{Acceptor}}\right|^*$$

Depletion voltage:

$$V_{\text{dep}} = \frac{eN_{\text{eff}}d^2}{2\varepsilon_0\varepsilon_r}$$

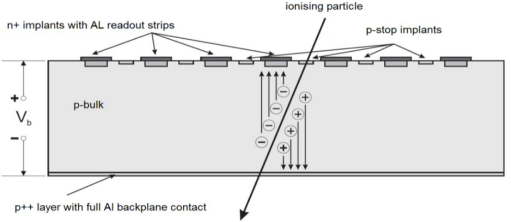

μ: Mobility
$\vec{E}$:El. field

d: Thickness
e: Elementary charge

ε_0: Vacuum permittivity
ε_r: Relative permittivity of Si

Wehner, Master Thesis, 2011

**Defects can act as donors or acceptors (important for irradiated sensors)*

Types of radiation damage

Two types of radiation damage in detector materials:

- **Bulk** (crystal) damage - Non Ionizing Energy Loss (NIEL)
  - Displacement damage/ crystal defects
  - Main focus of this study
- **Surface** damage - Ionizing Energy Loss (IEL)
  - Accumulation of charge in the $\mathrm{SiO_2}$ oxide, traps at the interface

Region affected by Ionizing Energy Loss (IEL) – Surface damage

Region affected by Non Ionizing Energy Loss (NIEL) – Bulk damage

M.Moll, Bethe Forum on Detector Physics 2014

Microscopic effects of NIEL

- 3 main mechanisms:
  - Coulomb elastic scattering (charged particles)
  - Nuclear elastic scattering
  - Nuclear inelastic scattering
- Dependence on energy of impact particle
- Point defects or defect clusters

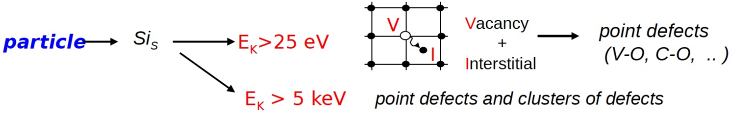

^{60}Co-gammas	Electrons	Protons	Neutrons (elastic scattering)
• Compton Electrons with max. $E_\gamma \approx 1$ MeV (no cluster production)	• E_e > 255 keV for displacement • E_e > 8 MeV for cluster		• E_n > 185 eV for displacement • E_n > 35 keV for cluster
Only point defects	**Point defects and clusters**	**Point defects and clusters**	**Mainly clusters**

M.Moll, Bethe Forum on Detector Physics 2014

Microscopic effects of NIEL

Simulation:

- Initial distribution of vacancies in $1\,\mu\mathrm{m}^3$ after $10^{14}\,\mathrm{particles/cm}^2$
- Keep in mind: The 'quality' of the damage depends on particle type and energy

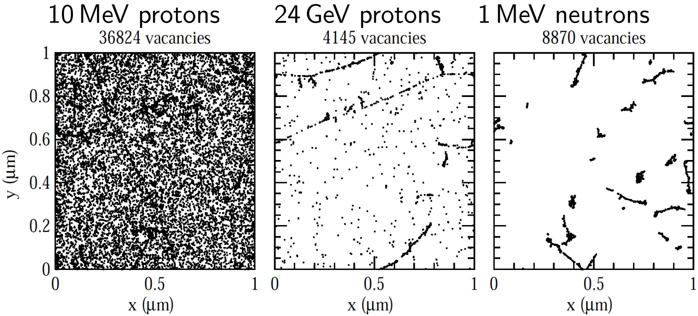

M.Huhtinen, Simulation of non-ionising energy loss and defect formation in silicon. NIMA, 491, 2002.

NIEL scaling hypothesis

Normalisation of radiation damage arising from different particles

$$\kappa = \frac{1}{D(1MeV\ neutrons)} \bullet \frac{\int D(E)\,\phi(E)\,dE}{\int \phi(E)\,dE}$$

- κ hardness factor of a radiation field (/monoenergetic particle) with respect to 1 MeV neutrons
- *D(E)* displacement damage cross section for a certain particle at energy *E*
- *D(1 MeV neutrons)* $=$ 95 MeVmb
- *f(E)* energy spectrum of the radiation field
- $\Phi(E)$ differential fluence at the energy E at the device level

Hypothesis: Damage function scales linearly with the NIEL

The integrals are evaluated for the interval $[E_{min}, E_{max}]$, with E_{min} and E_{max} being the minimum and maximum cut-off energy values, respectively, and covering all particle types present in the radiation field

Defects impact on detector properties

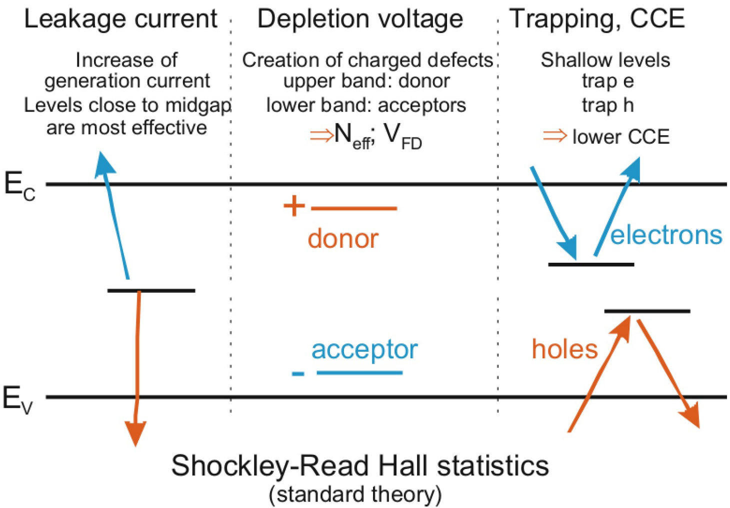

Annealing mechanisms

- **Migration and complex formation**
  - Defects become mobile at a certain temperature and can migrate through the silicon lattice
  - Migrating defects can for example recombine with their counterparts or form new defect complexes, e.g. $\mathrm{V} + \mathrm{O}_i \rightarrow \mathrm{VO}_i$
- **Dissociation**
  - A defect complex can decay into its components if the vibrational energy of the lattice is high enough
  - One or more of the constituents can migrate until forming another defect or disappearing into a sink

- All mechanisms need to overcome an energetic barrier: Activation energy
- All processes are temperature dependent

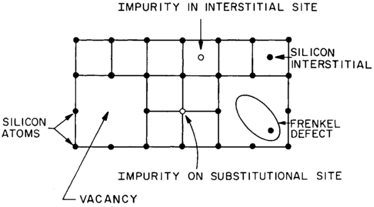

G. Lutz, Semiconductor radiation detectors, 2007

Macroscopic effects - Leakage current

Increase with fluence

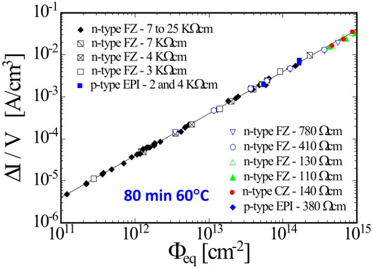

Decrease with annealing time

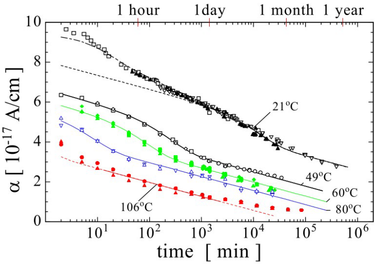

Current related damage factor

$$\alpha = \frac{\Delta I}{V\Phi_{eq}}$$

Current increase is independent of silicon production process (FZ, Epi, Cz) and impurity concentration types and concentration.

It can be a fluence indicator.

No reverse annealing for the leakage current.

Annealing is strongly temperature dependent.

M.Moll, Bethe Forum on Detector Physics 2014

Macroscopic effects - Depletion voltage

Change of effective doping concentration

with fluence Φ_{eq}

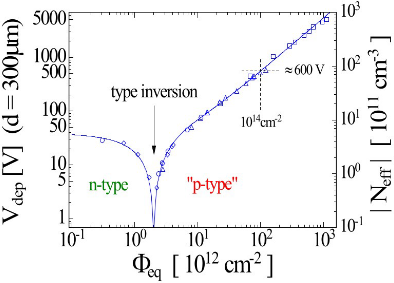

with annealing

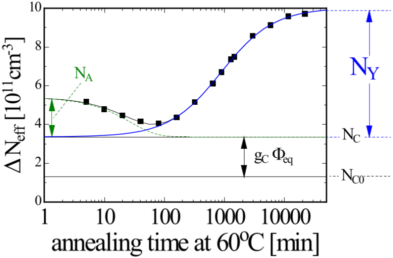

- For n-type sensors: Type inversion, N_{eff} changes from positive to negative, electric field building up from the backside
- Reason to change to p-type sensors at HL-LHC detectors

- Short term: Beneficial annealing
- Long term: Reverse annealing
- Time constants are temperature dependent
  → Detectors need to be cooled to avoid entering reverse annealing

M.Moll, Bethe Forum on Detector Physics 2014

Macroscopic effects - Trapping

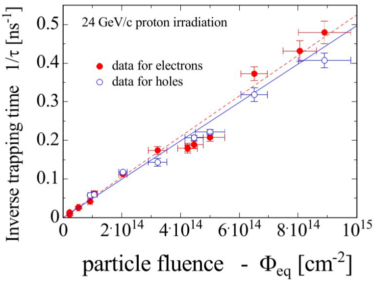

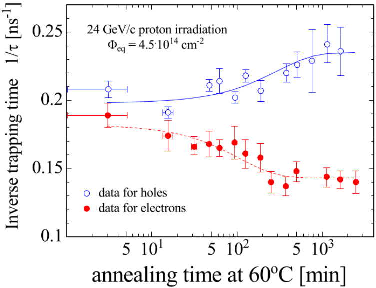

- Increasing inverse trapping time = increasing trapping probability
- Charge carrier trapping reduces the charge collection efficiency (CCE) at fixed collection time in irradiated sensors - limiting factor at high fluences
- Charge loss due to trapping is parameterized by inverse trapping time

M.Moll, Bethe Forum on Detector Physics 2014, Data from [Krasel 2004]

Summary - Radiation damage

- **Bulk damage** due to NIEL (diplacement defects)
  - Increase of leakage current - higher shot noise, thermal runaway
  - Increase of effective doping concentration - higher depletion voltages
  - Increase of charge carrier trapping - charge collection decrease
- **Annealing** effects
  - Leakage current decrease
  - Beneficial annealing dominates short term: Depletion voltage decrease, charge collection increase
  - Reverse annealing dominates long term: Depletion voltage increase, charge collection decrease

Introduction to HGCAL

- CMS will replace Calorimeter Endcaps (CE) for HL-LHC operation
- CE to be implemented in HGCAL (High Granularity Calorimeter) concept
- Silicon sensors will be used for the electromagnetic section and high radiation regions of the hadronic section of the CE
- $\sim$620 m^2 silicon sensors produced on 8-inch wafers (3x area of ATLAS tracker)

Key Parameters:
Coverage: $1.5 < |\eta| < 3.0$
~215 tonnes per endcap
Full system maintained at -30°C
~620m^2 Si sensors in ~26000 modules
~6M Si channels, 0.6 or 1.2cm^2 cell size
~370m^2 of scintillators in ~3700 boards
~240k scint. channels, 4-30cm^2 cell size
Power at end of HL-LHC:
~125 kW per endcap

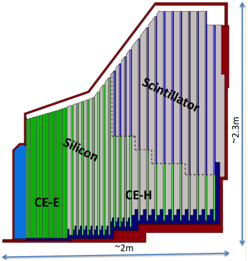

Introduction to HGCAL

- 3 different thicknesses: 300 μm, 200 μm (Float zone) and 120 μm (Epitaxial) - thinner sensors in high fluence regions
- Fluences of up to 1e16 n_{eq}/cm^2

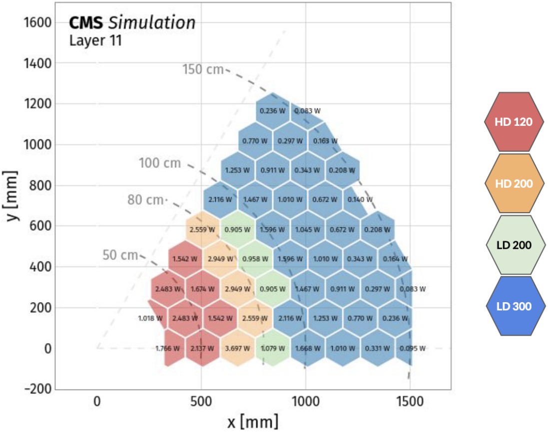

- 2 granularities: High and Low Density
- Hexagonal sensors: Optimal wafer usage and tiling

Silicon test structures: Diode measurements

- Hexagonal sensor from circular wafer
- Remaining space used for small sized test structures, e.g. diodes
- 8-inch wafers (20 cm), diodes with $0.5 \times 0.5\,\mathrm{cm}^2$ active area

Full wafer silicon sensor

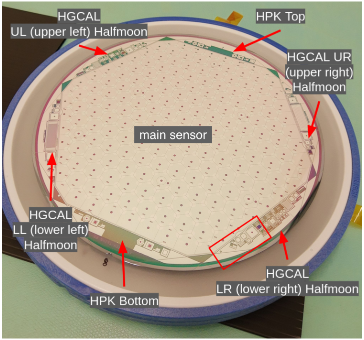

Test-structure diode contacted using two needles (pad and guardring)

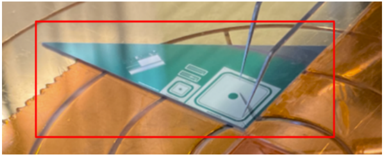

Irradiation campaign goals

Up to which fluence can we use which thickness

→ Does the charge collection follow the expected linear trend?

→ How does the leakage current and noise evolve with fluence?

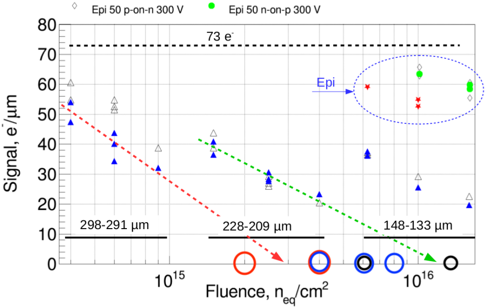

New campaign: O 300 µm, O 200 µm, O 120 µm

E. Curras Rivera, PhD Thesis 2017, HGCAL TDR

Which operation scenarios of HGCAL are feasible?

- Scintillators+SiPMs vs silicon sensors: temperature scenario needs to be good for both technologies
- Extraction of annealing time parameters at different temperatures
- Scaling factors between different annealing temperatures

High fluence irradiation campaign overview

- Test structures: Single pad diodes
- Neutron irradiation at JSI (Jozef Stefan Institute), Ljubljana, Slovenia
- 3 batches with 7 sensors each
- 3 annealing temperatures: 6.5°C, 20°C and 60°C - all ongoing!
- Leakage current and capacitance vs voltage (IV/CV) and charge collection (CC) measurement results

Test-structure diode on PCB

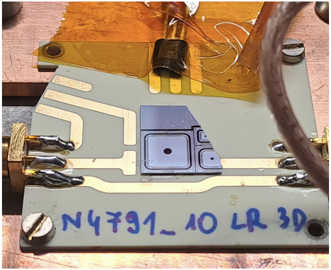

Sample overview per batch

Thickness\Fluence	2e15 n_{eq}\cm^2	4e15 n_{eq}\cm^2	6e15 n_{eq}\cm^2	8e15 n_{eq}\cm^2	1.5e16 n_{eq}\cm^2
300 um	X	X			
200um		X	X	X	
120um			X		X

Experimental setup: Early steps

- HGCAL needed setup for 24/7 annealing campaign
- Cover large phase space
  - Thickness (3)
  - Fluence (5)
  - Voltage (100-900 V)
  - Annealing time
  - Frequency

    ...
- Original version of Particulars setup after assembly (CC laser setup)
- Added cooling and humidity control → sensor box

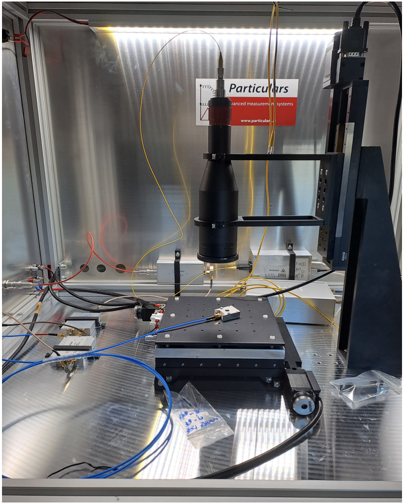

Co-funded by EP RD programme

Experimental setup: Early steps

- HGCAL needed setup for 24/7 annealing campaign
- Cover large phase space
  - Thickness (3)
  - Fluence (5)
  - Voltage (100-900 V)
  - Annealing time
  - Frequency

  …
- Original version of Particulars setup after assembly (CC laser setup)
- Added cooling and humidity control → sensor box

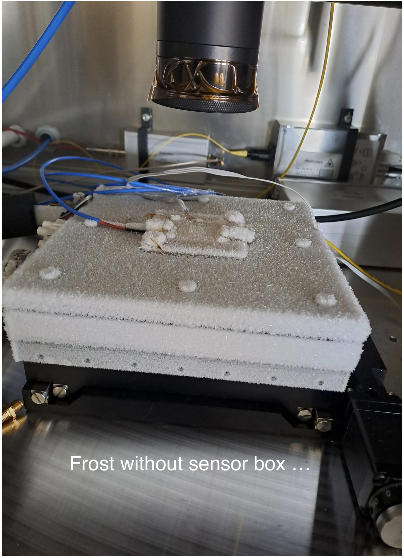

Experimental setup: Final version

- Upgraded it to IV+CV+CC setup
- Switchbox to change measurement type automatically
- Sensors are glued and wirebonded to a PCB, placed on a cooled copper holder, connected via SMA connectors

Particulars Setup

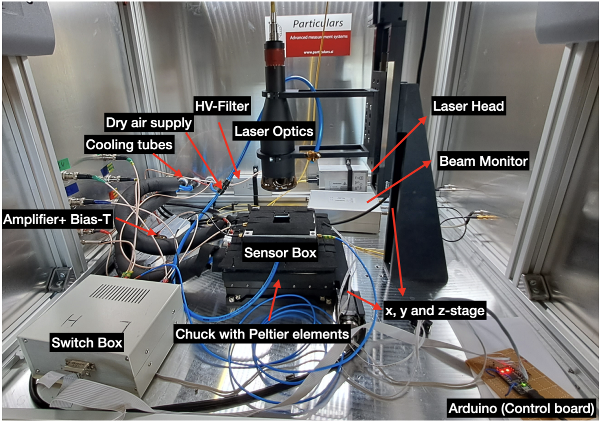

Leakage current vs fluence

- Initial = first post irradiation measurement = no additional annealing
- Expected increase with fluence
- Observe 10% leakage current difference in samples of same irradiation round, potentially linked to fluence inhomogenities along irradiation tube. Observed for the first time
- Offsets for different thicknesses - observed before (difference in electric field at same voltage)

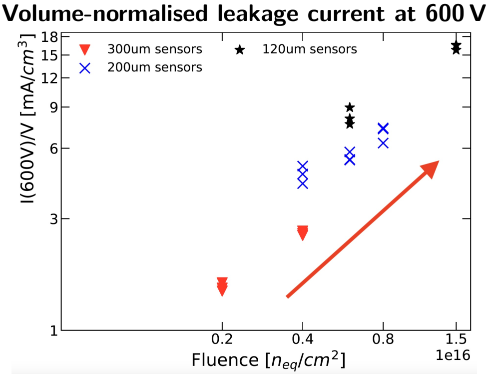

Saturation voltage from CV measurements

- Only extractable for thin sensors/ lower fluences without assumptions on saturation capacitance absolute value
- Frequency and temperature dependence - "saturation" instead of "depletion" voltage
- Further measurements all done at 2 kHz and −20°C

CV measurement example
120 µm, 6e15 n_{eq}/cm^2

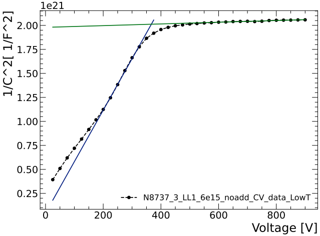

Frequency dependence

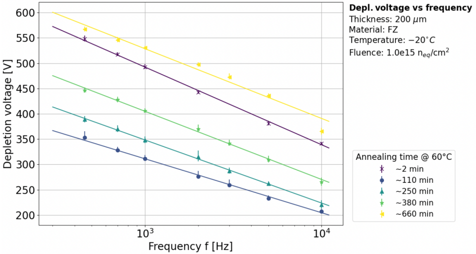

Saturation voltage vs fluence

- Small variance (10%) in extracted values
- In agreement with expected fluence variation (visible in leakage current)

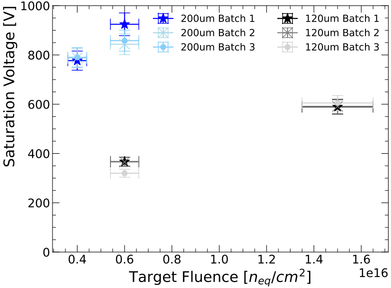

Saturation voltage vs fluence

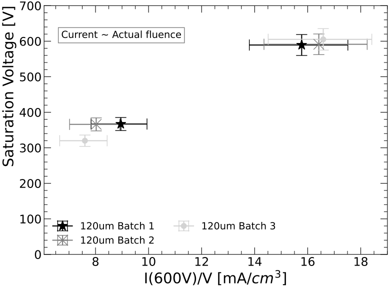

Saturation voltage vs current

Charge collection measurements

- Transient Current Technique (TCT): Infrared laser @1kHz from the top
- Laser calibrated to 40 MIP (Minimal Ionizing Particle) equivalent using unirradiated 300µm sample
- 300 events per voltage, each event average of 50 waveforms
- Integration over pulse → histogram → mean of Gauss-fit = Collected charge

Recorded waveform (averaged)

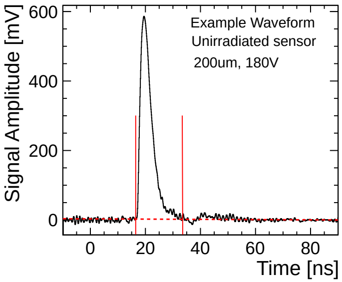

Charge collection histogram

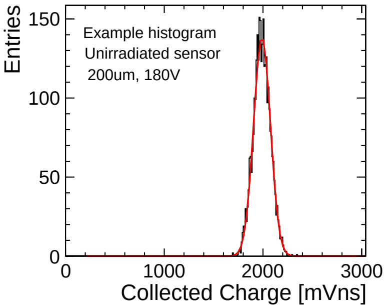

Charge collection measurements

Non-irradiated sensors

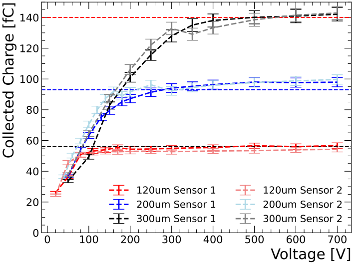

Used for crosschecks and reference measurements

Irradiated sensors

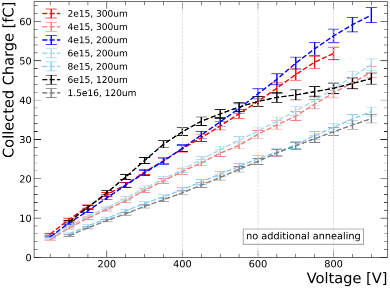

Further analysis focuses on charge collection and efficiency at specific voltages (400 V, 600 V, 800 V)

Dotted lines: Expected charge for different thicknesses

Charge collection vs fluence

- Without additional annealing for all 3 batches
- Expected decrease of charge with fluence (increased trapping probability)
- Efficiency = normalised by collected charge of unirradiated sensors
- Thinner sensors perform better at the same fluence despite lower starting values
- Very small variations in results between batches (<5%)

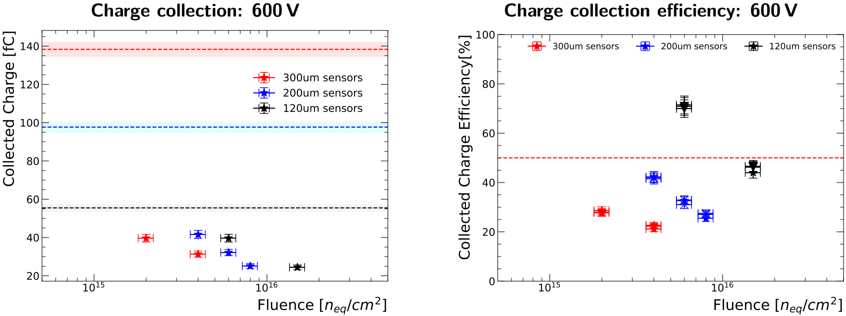

Charge collection: 600 V

Charge collection efficiency: 600 V

Dotted lines: Expected charge for unirradiated sensors/ 50% efficiency

Charge collection vs fluence

- Comparison with previous studies (measured in SSD group setup in 2021 and 2023)
- After 80-90 min annealing at 60°C
- Broad fluence range covered
- Results from different campaigns are well in agreement

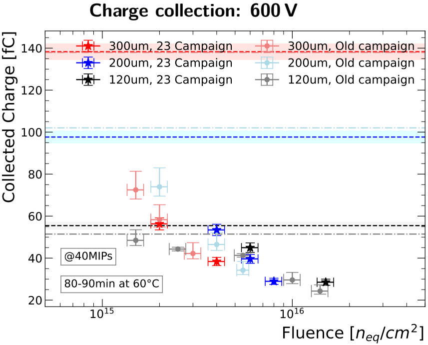

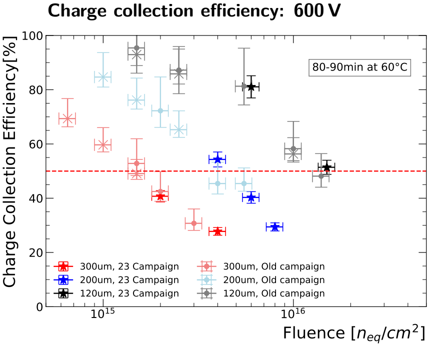

Dotted lines: Expected charge for unirradiated sensors/ 50% efficiency

Annealing behavior: Leakage current

- Volume-normalised leakage current at 600V
- Expected decrease for all annealing temperatures visible
- To be used to extract leakage current annealing time constant and temperature scaling factors once campaign is completed

6.5°C annealing

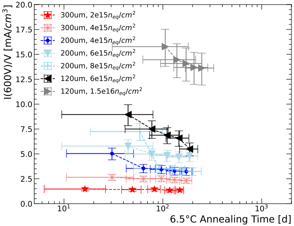

20°C annealing

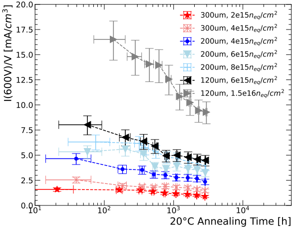

60°C annealing

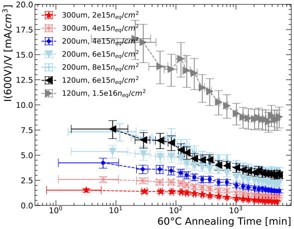

Annealing behavior: Saturation voltage

- Expected behavior for both temperatures: First decrease during beneficial and then increase during reverse annealing - increase of acceptor-like defects
- Difference in time scale clearly visible (hours vs minutes), 60°C annealing further progressed
- Directly correlates with the effective doping concentration

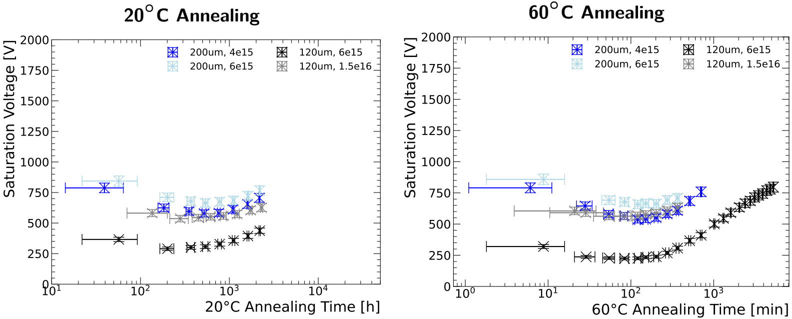

Annealing behavior: Charge collection

- 60°C annealing
- Expected increase of charge during beneficial annealing and expected decrease afterwards during reverse annealing
- The maximum seems to be reached around 110-120 min for FZ, 90 min for EPI - in agreement with other studies on p-type sensors
- At 600 V, there is a second bump for the 6e15 n_{eq}/cm^2 120 µm sensor

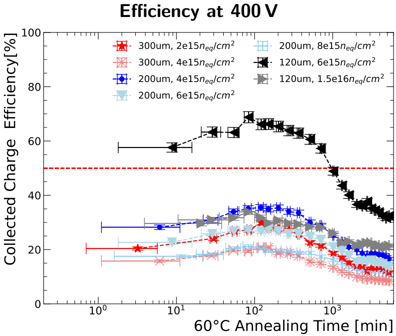

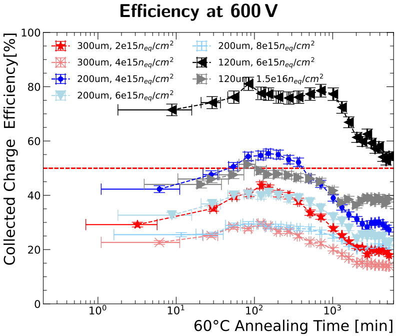

Annealing behavior: Charge collection

- No decrease of charge at 800 V for the 120 µm sensors
- Saturation/ increase again for higher fluences of the thicker sensors
- Electric field effects: As this is only present at higher voltages, it hints to the onset of some charge multiplication due to high electric fields - *Ongoing study, needs to be confirmed with further measurements*

Charge collection efficiency: 800 V

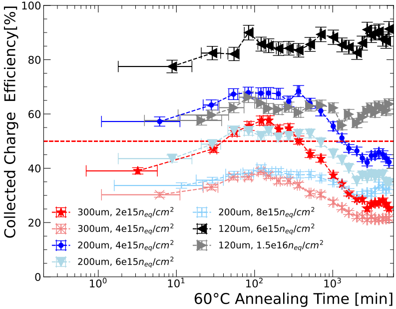

Charge collection efficiency: 120 µm sensors

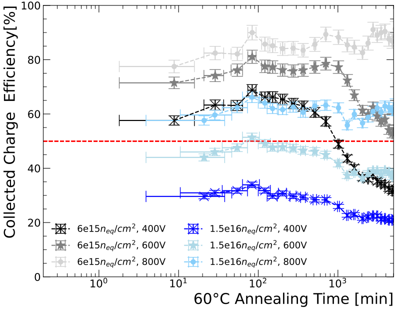

Dotted lines: Expected charge for 50% efficiency

Ongoing works

- Fits to access leakage current annealing time constant once enough data is recorded - *fluence variation might pose an issue for the fits*
- Fits to extract beneficial and reverse annealing time constants (CV) - need for more data during reverse annealing for both parameters - *limited data sets for saturation voltages might pose an issue for the fits*
- Extraction of scaling factors between annealing temperatures for both beneficial and reverse annealing*
- Comparison of the maximum charge increase during beneficial annealing for different temperatures*
- Comparison of the extracted minimum from CV measurements and maximum in charge collection at different temperatures*
- Comparison of proton and neutron irradiation damage: Proton irradiation campaign planned

**once enough data is recorded for lower temperatures*

Conclusions

- Ongoing broad annealing study covering a fluence range of 2e15 n_{eq}/cm^2 to 1.5e16 n_{eq}/cm^2 at 3 annealing temperatures: 6.5°C, 20°C and 60°C
- IV, CV and Charge Collection measurements done for each step
- Observed expected behaviour:
  - **Leakage current** increase with fluence, decrease with annealing
  - **Charge collection** decrease and **saturation voltage** increase with fluence
  - Beneficial annealing: Charge increase, saturation voltage decrease
  - Reverse annealing: Charge decrease, saturation voltage increase
- Further results, including the extraction of annealing time constants and scaling factors are expected within the upcoming months

Thank you for the attention

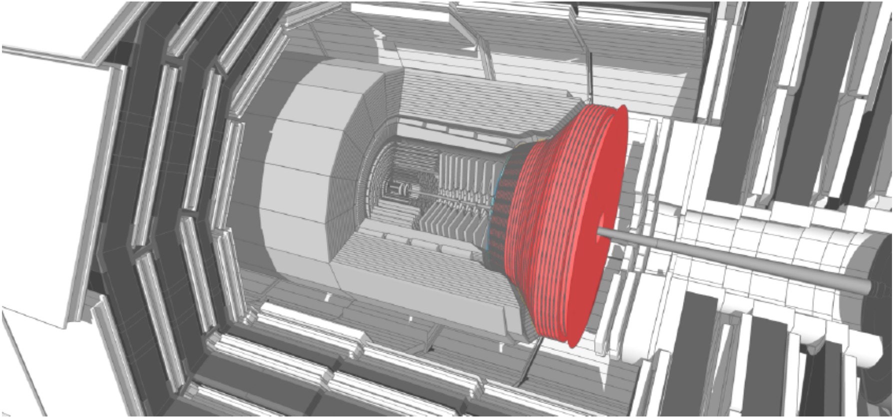

Backup

Irradiation at JSI Ljubljana

- Well established irradiation site used by RD50 community
- Same irradiation channel used for all test structure irradiations
- Estimation of fluence precision: within ±10%

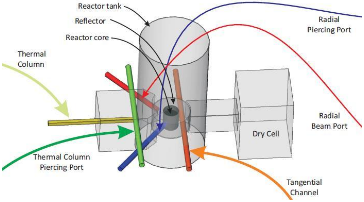

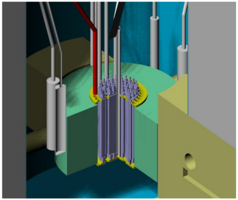

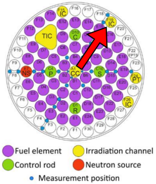

Hamburg model

Change of effective doping concentration with respect to before annealing:

$$\Delta N_{eff} = N_{eff,0} - N_{eff}(t)$$

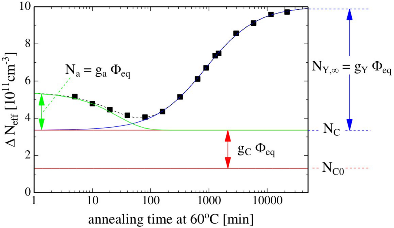

Long term reverse annealing

$N_Y(t) = g_Y \Phi_{eq}(1 - \exp(-t/\tau_Y))$

Build-up of acceptors during long-term annealing - first order process

$$N_{eff}(t) = N_A(t) + N_C + N_Y(t)$$

Short term annealing

$N_A(t) = g_a \Phi_{eq} \exp(-t/\tau_a)$

First order decay of acceptors introduced (proportional to Φ) during irradiation

Stable damage

$N_C = N_{C0}(1 - \exp(-c\Phi_{eq})) + g_c \Phi_{eq}$

Introduction of stable acceptors and incomplete "donor removal"

M.Moll, Bethe Forum on Detector Physics 2014

Initial results: Charge collection

- Higher charge at 800V than at 600V (Slide 9) as expected
- 120um sensors stay above 50% efficiency up to 1.5e16 n_{eq}/cm^2
- Slightly larger spread between sensors

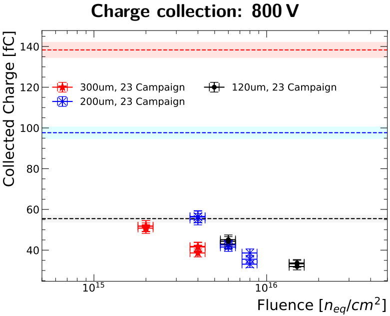

Charge collection: 800 V

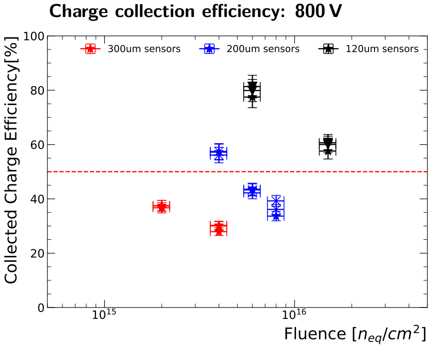

Charge collection efficiency: 800 V

Dotted lines: Expected charge for unirradiated sensors/ 50% efficiency

Charge comparison/Setup validation

Comparison of measurements at 600V after 80min annealing in two different setups

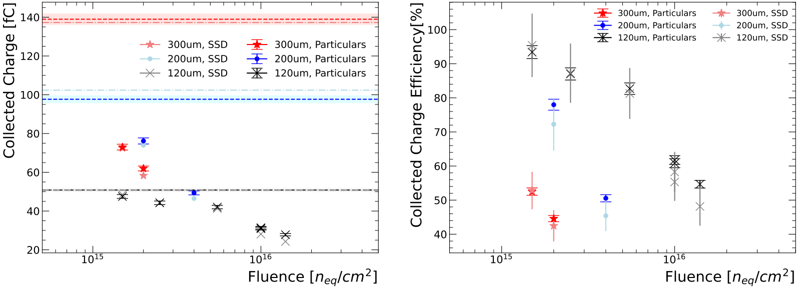

- Dotted lines represent unirradiated sensor measurements
- Results agree well within uncertainties between SSD and Particulars setups
- Measurement series used to validate a new Particulars-Setup as new standard IV/CV/TCT setup for upcoming campaigns

Annealing behavior: Charge collection

- 20°C annealing
- Expected increase of charge during beneficial annealing
- Start of decrease of charge during reverse annealing (ongoing measurements!)
- The maximum is harder to extract than for 60°C annealing - between 400-600h (16-25d)
- At 800V, for 120μm sensors no clear decrease

Efficiency at 400 V

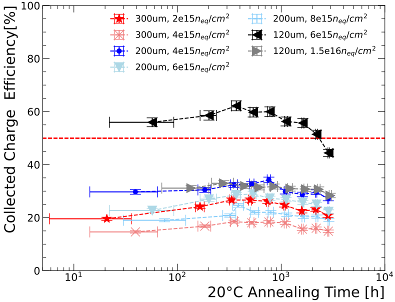

Efficiency at 800 V

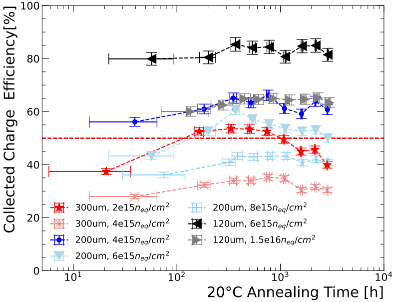

Annealing behavior: Charge collection

- 6.5°C annealing
- Expected increase of charge during beneficial annealing
- No clear start of decrease yet (ongoing measurement)
- Large uncertainty of the maximum beneficial annealing time (uncertain in-reactor annealing correction) - not clearly visible yet

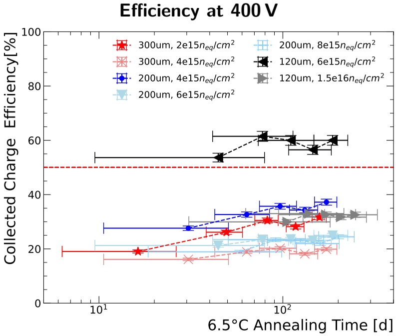
Efficiency at 400 V

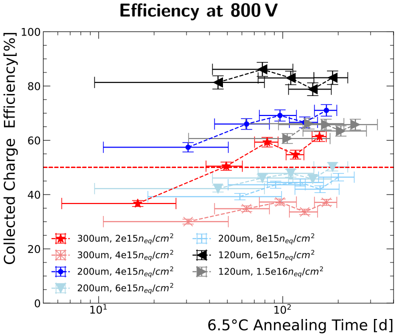
Efficiency at 800 V

Saturation voltage vs fluence

- Small variance (10%) in extracted values
- In agreement with expected fluence variation (visible in leakage current)

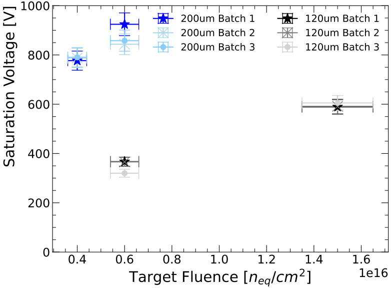
Saturation voltage vs fluence

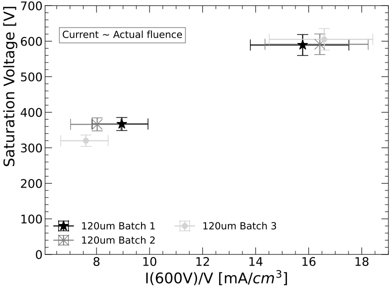
Saturation voltage vs current

Annealing behaviour: Damage parameter

- Extracted from leakage current vs fluence at each annealing step - $\frac{I}{V} = \alpha\Phi$
- Expected course: Decrease of damage parameter with annealing time
- Limited amount of samples and fluence uncertainty: Large uncertainties on extracted damage parameters

60°C annealing

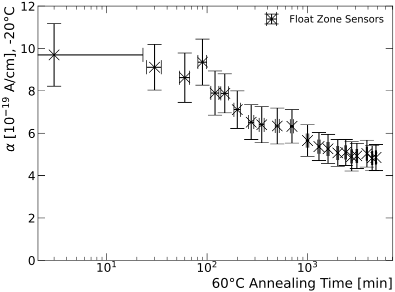

20°C annealing